Engineered Science
DOI: https://dx.doi.org/10.30919/es1258

Structural, Opto-Electronic and Transport Properties of Zintl Compound $YbZn_2Y_2$ (Y=P, As, Sb, Bi)

Tahir Amin,[1] Ali H. Reshak,[2, 3, 4,*] Zeshan Zada,[1] Inayat ur Rahman,[1] Dania Ali,[5] Shakeel Shakeel,[6] Abdul Munam Khan,[7] Amel Laref[8] and Muhammad M. Ramli[4]

Abstract

Structural, opto-electronic and thermoelectric properties of $YbZn_2Y_2$ (Y=P, As, Sb, Bi) compounds were determined by employing the full-potential linearized augmented plane wave plus local orbitals method (FPLAPW+lo). The modified Becke-Johnson exchange (mBJ) potential was adopted for the investigation of the band structures and the density of states. Through the mBJ technique, the compounds show metallic or semi metallic and semiconductor nature. In the total density of states (TDOS), the major participation is due to Yb-d and Yb-f states. Optical properties were determined in terms of real and imaginary parts of the dielectric function, refractive index, reflectivity, absorption coefficient, dielectric function and optical conductivity. It is evident that the $YbZn_2P_2$ compound shows the highest value of the figure of merit (ZT). The results indicate that these materials with strong thermoelectric capabilities are the most promising candidates for potentially effective optical and thermoelectric innovations.

Keywords: Opto-electronic; Thermoelectric; Zintl compound; Optical properties.
Received: 03 May 2024; Revised: 24 July 2024; Accepted: 10 September 2024.
Article type: Research article.

1. Introduction

In recent decades, thermoelectric materials (TEs) have attracted much attention in the scientific community due to their unique ability to convert heat directly into electrical energy without releasing harmful chemicals into the environment. The fundamental materials for power generation devices in thermoelectric (TE) technology, thermoelectric materials convert the waste thermal energy and solar energy into electrical energy without any additional energy consumption and are intensively investigated because of their numerous applications in industrial waste heat recovery, power generation, solid-state cooling and space technologies.[1-3] The term figure of merit (ZT) is used to describe the performance of TE material, and it is given by ZT = S2σT/κ, where S, σ, κ and T represent the Seebeck coefficient, the electrical conductivity, the thermal conductivity and *the* absolute temperature, respectively. The κ value usually emanates from two sources, i.e., the electronic contribution κe, which is proportional to σ based on the Wiedemann–Franz relationship, and the lattice contribution κl.[4,5] High-performance TE materials are estimated to retain low κ, and one of the actual solutions for high ZT is the exploration of alloy materials with inherently small κ values. On the other hand, the relation between S and σ is important because these parameters are coupled and generally work in reverse directions. The term "power factor (PF)" is defined as $S^2\sigma$, and a high PF is required to better describe the electronic and transport properties.[6] Zintl compounds have been reported as a good candidate for thermoelectric applications due to their distinctive characteristics. The complex crystal geometry and rich crystal chemistry make them responsive to

[1] *Material Modelling Lab, Department of Physics, Islamia College Peshawar, KP 25000, Pakistan.*
[2] *Physics Department, College of Science, University of Basrah, Basrah 61004, Iraq.*
[3] *Shatt Al-Arab University College, Basra, Iraq.*
[4] *Center of Excellence Geopolymer and Green Technology (CEGeoGTech), University Malaysia Perlis, Perlis, Kangar 01007, Malaysia.*
[5] *Faculty of medicine, Charles University, Pilsen 30100, Czech Republic.*
[6] *Faculty of Material Science and Engineering, Kunming University of Science and Technology, Kunming 650093, China.*
[7] *Department of Physics, RIPHAH International University Lahore, Lahore 45320, Pakistan.*
[8] *Department of Physics and Astronomy, College of Science, King Saud University, Riyadh 11451, Saudi Arabia.*
**Email:* maalidph@yahoo.co.uk (A. H. Reshak)

© Engineered Science Publisher LLC 2024

precise transport properties.[7,8] Zintl compounds, classified by their covalently bonded substructure, encircled by highly electropositive cations, have recently fascinated consideration due to their complex crystal structure.[9]

In the Zintl family, AB_2X_2 (A=Ca, Yb, Eu, Sr; B= Zn, Mn, Cd; X= Sb, Bi) type compounds show more attention due to their high thermoelectric efficiency [10-12] YbX_2Sb_2 (X= Mg, Zn, M and Cd) Zintl phases prepared by ball milling and hot pressing showed high thermoelectric performance.[13] The material that possesses a high S, high σ, and low κ should have a high thermoelectric performance.[14-16] These properties are closely consistent and even inconsistent with each other. In semiconductors, the S is high, while the carrier concentration is low. In metals, the σ is found to be high. The parameter κ consists of two parts: electronic part κe and lattice part κl, which have a great influence on ZT. Electronic thermal conductivity is closely related to electrical conductivity via the relation κe = LσT, where L is Lorenz number. The κl component is lattice thermal conductivity, which reflects the characteristics of phonon transport features, and it can be reduced without noticeably affecting the thermoelectric performance.[11,12,17] The transport properties of p-type Ba_2ZnX_2(X= Sb, As, Bi) were calculated by means of first principle calculation.[18] YbX_2Y_2 (X=Mg, Zn, Y= As, Sb, Bi) compounds have a tetragonal structure and belong to the Zintl family. A comprehensive study of these compounds is essential for exploring their potential for practical devices. In the present work, an extensive analysis of electronic, optical and thermoelectric properties is conducted using the density functional theory (DFT) framework. Generalized gradient approximation (GGA) and generalized gradient approximation plus Tran-Blaha modified Beck and Johnson (GGA-mBJ) potentials are used to provide a broad understanding of these compounds.[2,19] WIEN2k code is used for the electronic and optical properties, and BoltzTrap is used to calculate the thermoelectric properties. The optimized cell parameters are used for the calculations of structural, optical, and thermoelectric properties.

2. Computational methods

First-principles calculations based on DFT within the mBJ approximation, the full-potential augmented plane waves (FP-LAW+lo) method is implemented in the WIEN2K code.[20] The mBJ exchange and correlation energy of electrons were used to find out the Kohn Sham equation.[21] This is one of the most efficient and reliable methods to find out the ground-state properties based on DFT. To observe the structural relaxation, optimization, and enhanced accuracy of the band gap, we performed a modified Becke-Johnson exchange potential mBJ. Using Boltzmann transport theory,[22] the electrical conductivity, electronic thermal conductivity, Seebeck coefficient, and electronic transport coefficient can be easily investigated. Furthermore, the Boltzmann transport theory of phonons can be used to acquire the lattice thermal conductivity.[16] An acceptable degree of convergence was accomplished by analyzing a number of FP-LAW build functions up to the RMT Kmax = 8, where Kmax is the magnitude of the greatest K-vector, and RMT is the slightest radius of the muffin-tin spheres.

3. Results and discussion

3.1 Structural properties

Ternary Zintl compounds with the composition $YbZn_2Y_2$ (Y=P, As, Sb, Bi) and space group (No. 164) are predicted by using the volume optimization process (Fig. 1). Unit cell energy is minimized compared with fluctuations in the volume of the cell. At optimized volume, different structural parameters, such as lattice constant, ground state energy, unit cell volume, bulk modulus and its derivative, are obtained and listed in Table 1. The crystal structure for $YbZn_2X_2$ compounds is shown in Fig. 2.

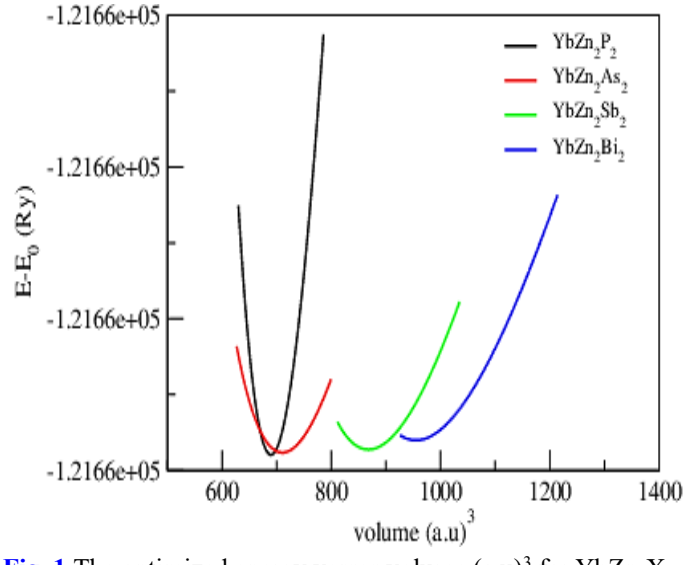

Fig. 1 The optimized energy verses volume $(a.u)^3$ for $YbZn_2X_2$ (X=P, As, Sb and Bi) compounds.

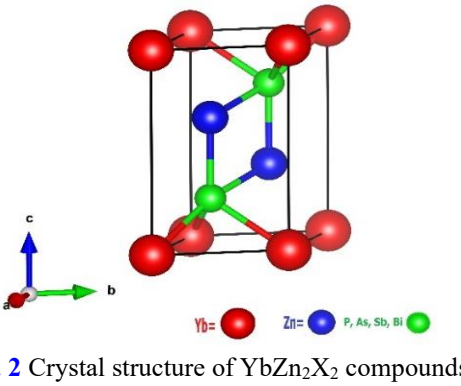

Fig. 2 Crystal structure of $YbZn_2X_2$ compounds.

© Engineered Science Publisher LLC 2024

Table 1. The structural parameters, a(Å), c(Å), the pressure derivative (B´), the Bulk Modulus B(GPa), the optimized volume V_o and the ground state Energy E_o along with its experimental values.

Compounds	a(A°)	c(Å)	a (Å)	c (A°)	V_o	B [GPa]	B´	E_o
	Calculated		Exp	Exp				
$YbZn_2P_2$	4.11	6.96			689.716	314.73	5.000	-36705.047925
$YbZn_2As_2$	4.16	7.02			710.779	64.621	5.000	-44380.927308
$YbZn_2Sb_2$	4.46	7.44	4.4424[c]	7.418[d]	868.2685	50.746	5.000	-61270.961542
$YbZn_2Bi_2$	4.67	7.49			956.707	44.043	5.000	-121662.530095

[c]Ref. [22],[d] Ref. [23].

3.2 Electronic properties

In this work, we perform a self-consistent calculation using the mBJ functional. We calculated the band structures in order to analyze the optical feedback of these materials. Through the technique of mBJ the $YbZn_2As_2$, $YbZn_2Sb_2$ and $YbZn_2Bi_2$ compounds show a metallic or semi metallic nature, and $YbZn_2P_2$ shows semiconductor nature with very small indirect energy gap (Table 2, Fig. 3). These materials are very suitable for thermoelectric applications. This surprising behavior may be due to the position of the *f*-state of Yb atom. Moreover, there appeared two valleys in Γ, M directions, which leads to a high-power factor (=$S^2\sigma$), as previously revealed.[21,22]

Table 2. The energy band gaps in $YbZn_2X_2$(X= P, As, Sb and Bi) compounds, as calculated using TB-mBJ.

Compounds	Eg (eV)
$YbZn_2P_2$	0.09
$YbZn_2As_2$	Metal
$YbZn_2Sb_2$	Metal
$YbZn_2Bi_2$	Metal

3.3 Density of states

The total densities of states (TDOS) and partial densities of states (PDOS) of the YbX_2Y_2 compounds (X = P, As, Sb, and Bi) are presented in Fig. 4. As obtained using the TB-mBJ functional. It is seen that in all compounds, the main contribution is the *f*-states of the Yb atom. If the graphs are observed carefully, then it is seen that the main contribution in the conduction band is due to Yb-*d* states and Zn atoms. In contrast, in the valence band, the dominant contribution is of Yb-*f* states and pnictogen group (X = P, As, Sb, Bi) atoms, with very little contribution from the Zn atom.

3.4 Optical properties

The $YbZn_2X_2$ (X= P, As, Sb and Bi) compounds might be promising solar cell absorbents. To investigate the possibility, we calculated the important optical properties, including complex dielectric function, reflectivity, complex refractive index, reflectivity and optical conductivity of the understudied materials. The complex dielectric function is expressed below.[24]

$$\varepsilon(\omega) = \varepsilon_1(\omega) + i\varepsilon_2(\omega) \quad (1)$$

The frequency-dependent polarization and absorption of a material are characterized and quantified in terms of the dielectric function ε(ω). The real part, $\varepsilon_1(\omega)$, describes the material's electric polarization in response to an external electric field. The Kramers-Kronig equation is utilized to compute this real part.[24]

$$\varepsilon_1(\omega) = 1 + \frac{2}{\pi} P \int_0^{\infty} \frac{\acute{\omega}\varepsilon_2(\acute{\omega})}{\acute{\omega}^2 - \omega^2} d\omega \quad (2)$$

Identification of the frequency-dependent imaginary part, $\varepsilon_2(\omega)$, within the equation allows for the inference of the absorptive behavior of the material. [25] Subsequently, the frequency-dependent $\varepsilon_2(\omega)$ in crystals with cubic symmetry is expressed as: [26]

$$\varepsilon_2(\omega) = \frac{8}{2\pi\omega^2} \sum_{nn} \int_{BZ} |P_{nn}|(k)^2 \frac{dS_k}{\nabla\omega_{nn}(k)} \quad (3)$$

The dipole matrix element, denoted as $|P_{nn}(k)|$, signifies the transition between the first and last states, with S_k representing the constant value in terms of energy surfaces, and ω_{nn} (k) representing the energy difference between the two states. These optical properties play a crucial role in the design and development of optical devices.[27,28] The calculated real and

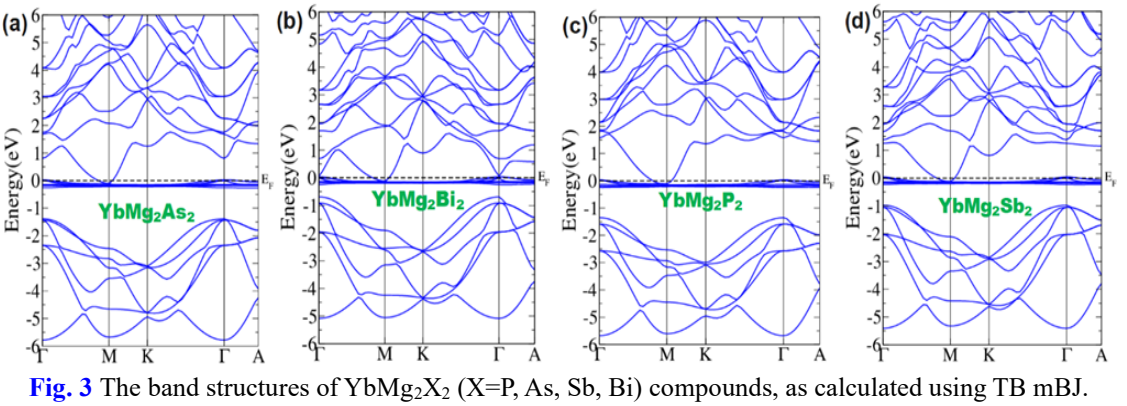

Fig. 3 The band structures of $YbMg_2X_2$ (X=P, As, Sb, Bi) compounds, as calculated using TB mBJ.

© Engineered Science Publisher LLC 2024

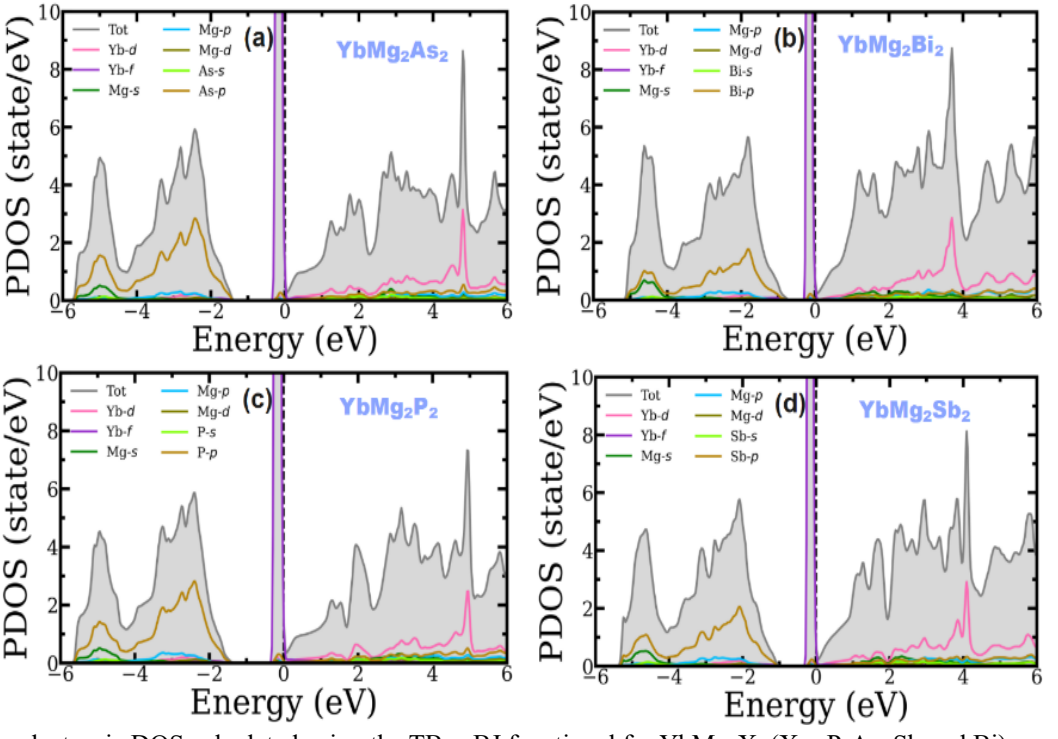

Fig. 4 The electronic DOS calculated using the TB-mBJ functional for $YbMg_2X_2$ (X = P, As, Sb and Bi) compounds.

imaginary parts of the dielectric function are given in Fig. 5(a) and (b), which identify the optical dielectric response function for $YbZn_2X_2$ (where X belongs to the pnictogen family) compounds in the energy range of 0 to 10 eV. Also, the maximum values for the real and imaginary parts of the dielectric function are determined. In Fig. 5a are the static dielectric functions ε1 (0) rise from $YbZn_2P_2$ to $YbZn_2Bi_2$ as expected. Sharp peaks of ε1 (ω) are noted for $YbZn_2P_2$, $YbZn_2As_2$, $YbZn_2Sb_2$ and $YbZn_2Bi_2$, which are to be 16.50, 14.20, 17.50 and 22.01 at energy points 3.11, 3.03, 2.68 and 2.08 eV from P to Bi, respectively. The energy ranges of the studied compounds occur in the visible region of the spectrum. However, in Fig. 5(a), it is difficult to find 17.50 and 22.01 at 2.68 and 2.08 eV. In Fig. 5(b), we display the imaginary part $\varepsilon_2(\omega)$ of the optical dielectric function as a function of energy, which is the sum of total ground state transitions from the occupied states of the VB to the unoccupied states of the CB. These spectra start from the fundamental transition edge, which is the excitation of electrons from the maximum of the valence band to the minimum of the conduction band. This fundamental transition is called the threshold point. Beyond this point, the curve increases sharply due to large interband transitions.

The refractive index is the ratio between the speed of light in a vacuum and the speed of light in a medium. The calculated dispersive refractive index of $YbZn_2X_2$ (X = P, As, Sb and Bi) compounds is shown in Fig. 6. The curves follow the real parts of dielectric functions. At zero frequency, the refractive index values n (0) is 4.0 at 3 eV for $YbZn_2P_2$, 4.1 at 2.9 eV, for $YbZn_2As_2$, and 4.7 at 2.8 eV, for $YbZn_2Sb_2$. However, the refractive index of $YbZn_2Bi_2$ is from its starting point, *i.e.*, 6.1, due to the modified extra metallic transition.

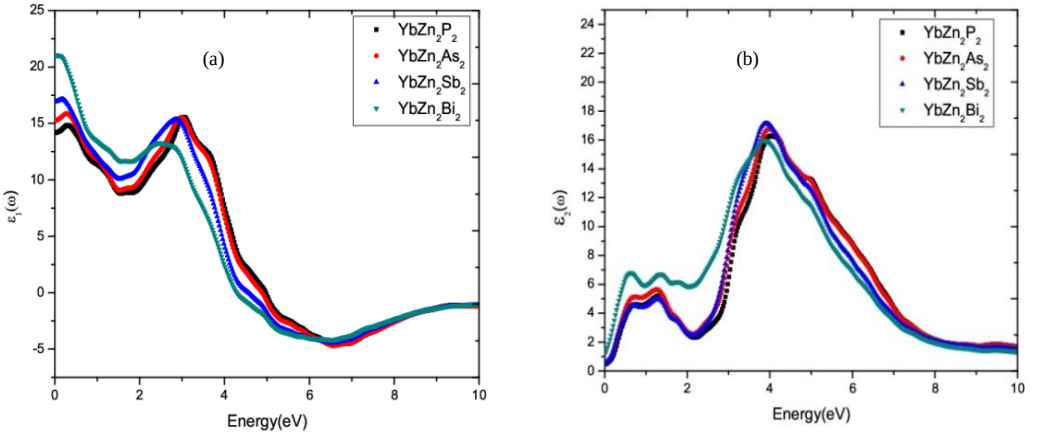

Fig. 5 The calculated (a) Real ε1(ω) and (b) Imaginary ε2(ω) parts of dielectric functions of the $YbZn_2X_2$ (X= P, As, Sb, Bi) compounds.

© Engineered Science Publisher LLC 2024

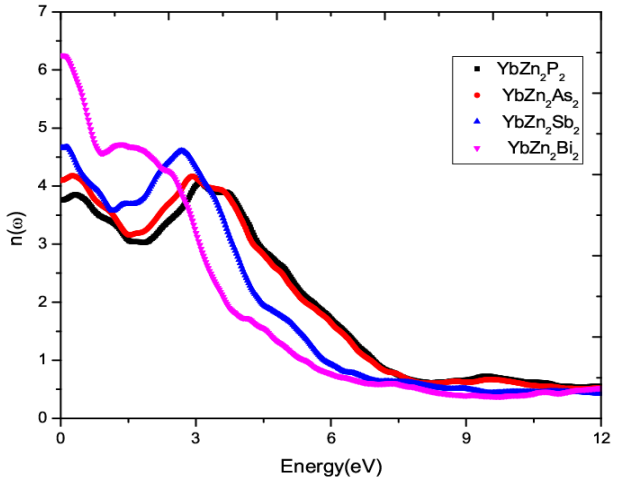

Fig. 6 Dispersive refractive index obtained for $YbZn_2X_2$ (X=P, As, Sb, Bi) compounds.

When light falls on a metal surface, it increases the energy of the electrons on the surface, and the photons are absorbed inside the metal. The absorption coefficient I (ω) relates the incident and absorbed photons. Fig. 7 points out the interaction and absorption of photons within a material. Looking carefully into the figure, the absorption coefficient greatly affects the incident photon, which increases with increasing incident photon energy. For (Zn) base elements of our present research compounds, the plots indicate that the highest value of absorption coefficient for the zinc (Zn) compounds $YbZn_2X_2$ (X= P, As, Sb and Bi) are plotted. The highest peaks for $YbZn_2P_2$, $YbZn_2As_2$, $YbZn_2Sb_2$ and $YbZn_2Bi_2$ compounds are 9000 cm^{-1}, 70600 cm^{-1}, 10900 cm^{-1}, 90400 cm^{-1}, respectively. The reflectivity (R(ω)) can be mathematically expressed in terms of $\varepsilon_1(\omega)$ and $\varepsilon_2(\omega)$ as given below.[29-31]

$$n(\omega) = \frac{1}{\sqrt{2}}[\{\varepsilon_1(\omega)^2 + \varepsilon_2(\omega)^2\} + \varepsilon_1(\omega)\,]^{1/2} \quad (4)$$

$$k(\omega) = \frac{1}{\sqrt{2}}[\{\varepsilon_1(\omega)^2 + \varepsilon_2(\omega)^2\} - \varepsilon_1(\omega)\,]^{1/2} \quad (5)$$

$$R = \frac{(n-1)^2+k^2}{(n+1)^2+k^2} \quad (6)$$

The reflectivity (R) is influenced by the refractive index (n) and extinction coefficient (k) of the material, as evident from the aforementioned equation. This implies that the reflectivity is affected by the speed at which electromagnetic radiation propagates within the material, as well as the rate at which the incident electric field amplitude decays or is damped.

Reflectivity is basically the optical property of a material, which is the intensity ratio of an incident and reflecting light. Reflectivity R(ω) (Fig. 8) details a material's surface properties. For Zintl compounds at zero frequency reflectivity R(0), the reflection found is 34%, 36%, 42% and 53%, while the values of reflectivity R(ω) are 54%, at 7.5 eV, 54% at 7.4 eV, 60% at 5.9 eV, and 58% at 4.0 eV for $YbZn_2P_2$, $YbZn_2As_2$, $YbZn_2Sb_2$, and $YbZn_2Bi_2$. As clear from the curves, these compounds have high thermoelectric properties in regions with high reflectivity due to their potential to avoid solar heating. The optical parameters obtained for Zintl compounds $YbZn_2Y_2$ (X=P, As, Sb, Bi) are shown in Table 3.

4. Transport properties

For the studied compounds, we evaluated the thermoelectric transport properties to investigate how waste heat transformed into useful electrical energy. For this purpose, we used the Boltz TraP code interfaced to WIEN2K to determine the essential transport quantities, such as electrical conductivity (σ), Seebeck coefficient (S), thermal conductivity (κ), power factor ($S^2\sigma$) and dimensionless thermoelectric figure of merit (ZT), as a function of temperature. BoltzTraP code uses the semi classical transport theory[21] with all the same optimized parameters to calculate the transport quantities. Thomas Seebeck depicted that when there is a temperature gradient in some distinct materials, this temperature gradient will result in an emf.

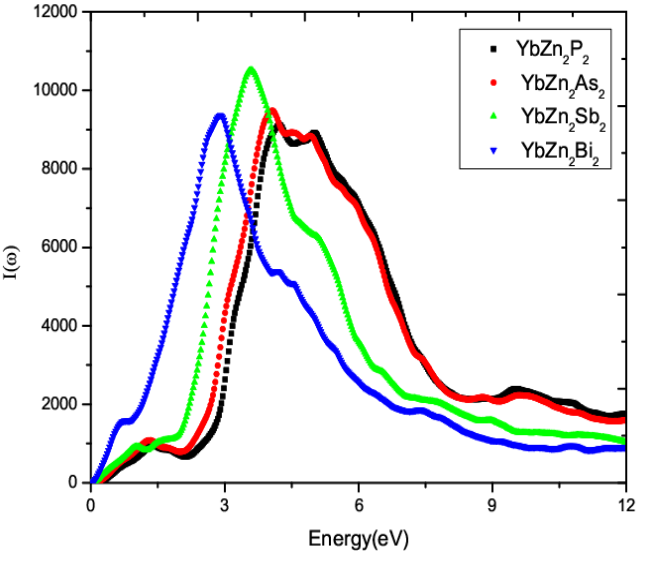

Fig. 7 The interaction and absorption of photons within the materials are pointed out.

Table 3. Optical parameters for Zintl compounds $YbZn_2Y_2$ (X=P, As, Sb, Bi).

Compounds	Dielectric		Refractive index (n)	Reflectivity R(ω)%	Conductivity $\sigma(\omega)_{max}$ $\Omega^{-1}cm^{-1}$	Absorption Coefficient $\alpha(\omega)_{max}cm^{-1}$
	ε_{1max}	ε_{2max}				
$YbZn_2P_2$	16.50	3.9	3.6	54	80500	9000
$YbZn_2As_2$	14.20	3.8	4.1	54	80700	70600
$YbZn_2Sb_2$	17.50	3.7	4.6	60	10200	10900
$YbZn_2Bi_2$	22.01	3.6	6.2	58	80650	90400

© Engineered Science Publisher LLC 2024

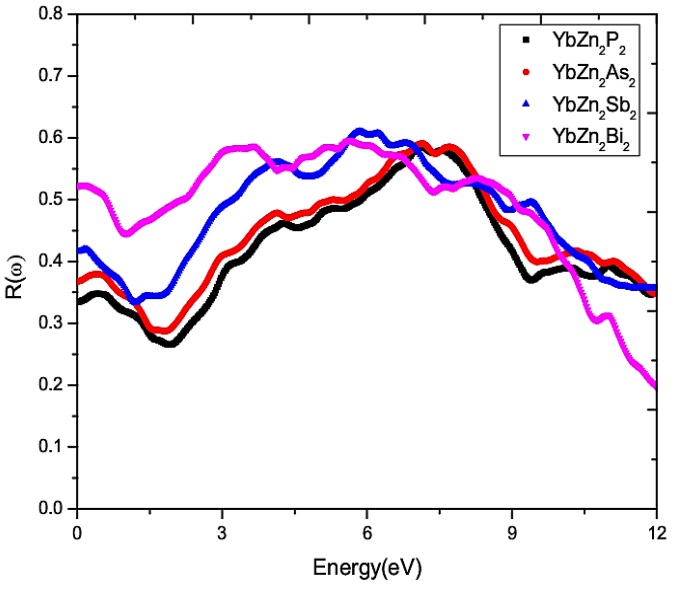

Fig. 8 Reflectivity spectra versus incident photon energy for $YbZn_2X_2$(X=P, As, Sb, Bi) compounds.

4.1 Electrical conductivity

Electrical conductivity (σ) best explains the conductor or semiconductor nature of a compound having an excess of free electrons. Providing thermal energy, excites free electrons, and as a result, the material starts conduction. The calculated σ of the investigated compounds is shown in Fig. 9. The σ of $YbZn_2X_2$ (X= P, As, Sb, Bi) has been drawn per relaxation time against temperature on the horizontal axis. At a temperature of 300K (room temperature), most of the compounds have the minimal value of σ, while at a temperature of 800 K, all the compounds show maximal σ. The values noted for Zintl compounds are quite different from the previous ones and are also shown in the plot. Again, at room temperature 300 K, all the compounds have minimum values except $YbZn_2P_2$, which has a maximum value different than the values of $YbZn_2As_2$, $YbZn_2Sb_2$, and $YbZn_2Bi_2$ compounds, as noted in the plot which is (0.0×10^{201}, 0.5×10^{18}, 5.0×10^{20}, and 2.4×10^{20}) Ω. m. s^{-1}.

4.2 Seebeck Coefficient (S)

Seebeck coefficient is also called thermopower or thermoelectric sensitivity of a material. It shows the magnitude of an induced thermoelectric voltage in response to temperature differences within the material. The Seebeck coefficient is negative for negative charge carriers (electrons) and positive for positive charge carriers. The calculated S as a function of temperature is shown in Fig. 10. All the samples show negative S values over the full temperature range of 300–1000 K. It is obvious from the curves that the S value for the compounds mentioned above is significantly varied with an increase in temperature. At 300 K, the calculated S values are -2.4×10-5 μV/K, 1.5×10-5 μV/K, -0.5×10-5 μV/K and -3.5×10-5 μV/K for $YbZn_2P_2$, $YbZn_2As_2$, $YbZn_2Sb_2$ and $YbZn_2Bi_2$ respectively.

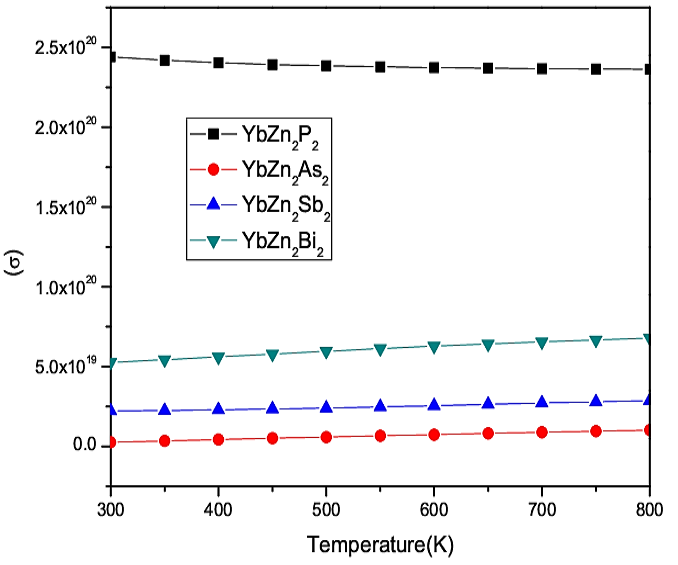

Fig. 9 Electrical conductivity obtained for $YbZn_2X_2$(X=P, As, Sb, Bi) compounds.

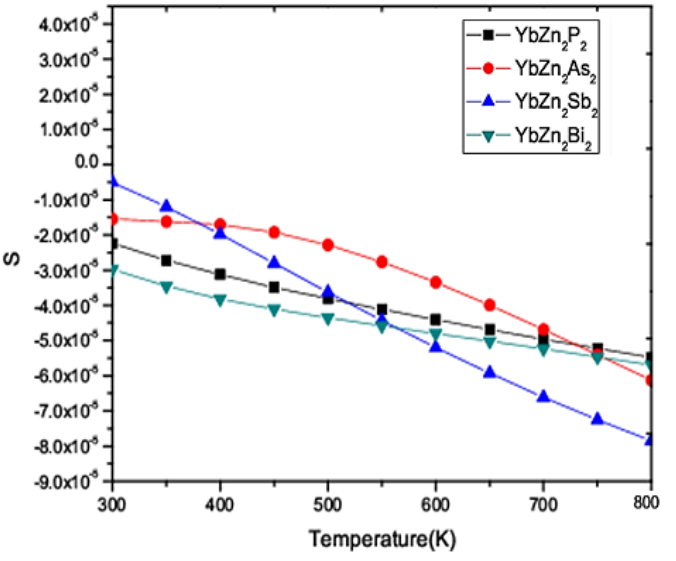

Fig. 10 Seebeck coefficient as a function of temperature in $YbZn_2X_2$ (X=P, As, Sb, Bi) compounds.

4.3 Thermal conductivity

Thermal conductivity is represented by (κ). It is a temperature dependent thermal quantity of a material. The κ level greatly varies with the changes in temperature. Thermal conductivity indicates how well a material conducts heat, determining whether it is a good conductor or an insulator. A material is first tested with this behavior and then used for many thermal applications, like a material with high κ being used in a heat sink, while a material with low κ is used for heat insulation. In Fig. 11, the changes of κ against temperature are shown for

 © Engineered Science Publisher LLC 2024

Zintl compounds under consideration. At 300K, the values are 0.2×1015, 0.7×1015, 1.5×1015, and 4.65×1015, for $YbZn_2As_2$, $YbZn_2Sb_2$, $YbZn_2Bi_2$ and $YbZn_2P_2$, respectively.

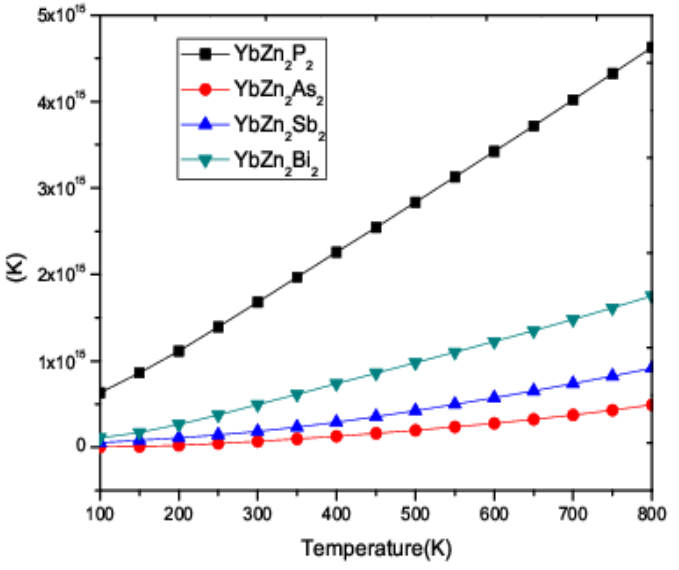

Fig. 11 Thermal conductivity for $YbZn_2X_2$ (X = P, As, Sb, Bi) compounds.

4.4 Figure of merit (ZT)

The efficiency of thermoelectric devices is simply known as the figure of merit (ZT). It shows the effectiveness or power generation of thermoelectric devices.

To quantify ZT, the following equation is used:

$$ZT = \frac{\sigma S^2 T}{K} \quad (7)$$

This equation shows that the figure of merit of a material depends on the following factors:

- Electrical conductivity (σ)
- Seebeck coefficient(S^2)
- Temperature (T)
- Thermal conductivity (K).

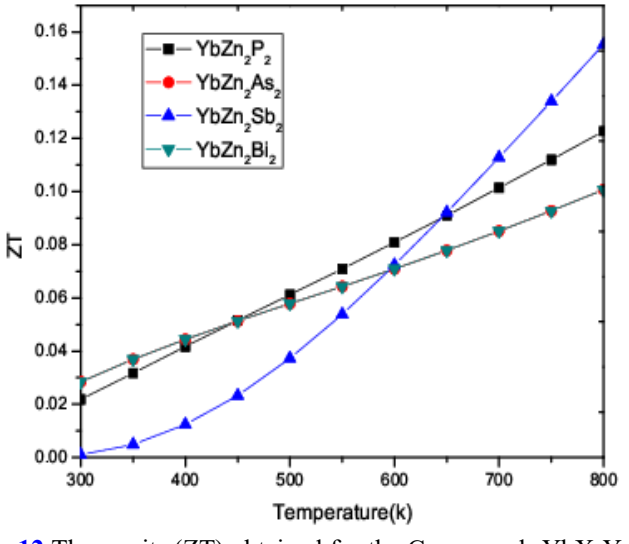

Fig. 12 The merits (ZT) obtained for the Compounds YbX_2Y_2(X = Zn; Y= P, As, Sb, Bi)

Figure 12 shows the variation of ZT for $YbZn_2X_2$ (X = P, As, Sb, and Bi) compounds with temperature. The figure of merit ZT for compounds $YbZn_2P_2$, $YbZn_2As_2$ linearly increases with increasing the temperature, while $YbZn_2Sb_2$, and $YbZn_2Bi_2$ gradually increase with a rise in temperature. The calculated figure of merit (ZT) values for $YbZn_2P_2$, $YbZn_2As_2$, $YbZn_2Sb_2$, and $YbZn_2Bi_2$, are 0.00, 0.021, 0.03 and 0.04 respectively. The ZT values increase for Zn compounds as we move from phosphorus to bismuth down in the ncitogen family at 300 K.

5. Conclusions

The structural, optical, electronic and thermoelectric properties of the $YbZn_2Y_2$-type compounds are determined by first-principal calculations using the full-potential linearized augmented plane wave (FP-LAPW) within the Wien2k code. Generalized gradient approximation (GGA) was used to optimize the unit cell volume. It is concluded from the optimization of structure that these compounds show trigonal geometry and lattice constants that are very close to the experimental outcome. The electronic band structure calculations were used to find out the nature of the nature of the materials. The density of state (DOS) showed that in these compounds, the *p*- (P, As, and Sb) states are situated in the conduction band, while *the d*- (Yb) state contribution is dominant, with a small part of *the p*-states of P, As, and Sb. The optical behavior of these compounds is determined here in terms of complex dielectric function, refractive index, extinction coefficient, optical conductivity, absorption, and reflectivity. The maximum refractive index value is obtained for $YbZn_2Bi_2$. The reflectivity obtained for these compounds is about 60%, making them suitable candidates for shielding purposes. The thermoelectric behavior of $YbZn_2Sb_2$ compounds shows high thermoelectric efficiency, indicated by high values of the figure of merit (ZT). These compounds exhibit frequent changes in ZT values with increasing temperature, while the rest of the compounds show no major changes in ZT values. These materials with high ZT values are of great importance in thermoelectric applications. Due to this property, $YbZn_2As_2$ can be used in heat sink applications, while other compounds $YbZn_2Y_2$ (Y=P, Sb, Bi) with lower values of ZT can be used for insulation functions because of their low thermal conductivity.

Acknowledgment

This research project (for A. Laref) was supported by a grant from the "Research centre of the Female Scientific and Medical Colleges", Deanship of Scientific Research, King Saud University.

© Engineered Science Publisher LLC 2024

Conflict of Interest

There is no conflict of interest.

Supporting Information

Not applicable.

References

[1] M. D'Angelo, C. Galassi, N. Lecis, Thermoelectric materials and applications: a review, *Energies*, 2023, **16**, 6409, doi: 10.3390/en16176409.

[2] Z. Zada, A. A. Khan, A. H. Reshak, A. M. Khan, S. Shakeel, D. Ali, M. Ismail, M. M. Ramli, A first principles study of Palladium-based full Heusler ferromagnetic Pd_2MnSb compound, *Optical and Quantum Electronics*, 2023, **56**, 248, doi: 10.1007/s11082-023-05463-8.

[3] M. Mukherjee, A. Srivastava, A. K. Singh, Recent advances in designing thermoelectric materials, *Journal of Materials Chemistry C*, 2022, **10**, 12524-12555, doi: 10.1039/d2tc02448a.

[4] A. Dadhich, M. S. Ramachandra Rao, K. Sethupathi, Physics and technology of thermoelectric materials and devices, *Journal of Physics D: Applied Physics*, 2023, **56**, 333001, doi: 10.1088/1361-6463/acc9d0.

[5] Z. Zada, J. Khan, A. A. Khan, A. H. Reshak, D. Ali, F. U. Rehman, I. Urrahman, M. Saqib, M. Irfan, M. M. Ramli, Structural, thermoelectric, electronic, and magnetic properties of pristine intermetallic rare-earth-based XMn_2Si_2 (X=Dy, Er) compounds, *ECS Journal of Solid-State Science and Technology*, 2023, **12**, 043012, doi: 10.1149/2162-8777/acccaa.

[6] M. Wolf, R. Hinterding, A. Feldhoff, High power factor *vs.* high zT—a review of thermoelectric materials for high-temperature application, *Entropy*, 2019, **21**, 1058, doi: 10.3390/e21111058.

[7] J. Shuai, J. Mao, S. Song, Q. Zhang, G. Chen, Z. Ren, Recent progress and future challenges on thermoelectric Zintl materials, *Materials Today Physics*, 2017, **1**, 74-95, doi: 10.1016/j.mtphys.2017.06.003.

[8] Z. Zada, A. A. Khan, A. H. Reshak, I. Khan, S. Zada, M. Ismail, M. Fazal-ur-Rehman, M. Saqib, G. Murtaza, Q. Khan, M. M. Ramli, Insight into the electronic structure, magnetic, and thermoelectric properties of transition metal pnictides KCr2L2 (K= Ca, Sr; L = P, As): As substitute source for renewing energy, *Physica B: Condensed Matter*, 2023, **649**, 414470, doi: 10.1016/j.physb.2022.414470.

[9] J. A. Cooley, P. Promkhan, S. Gangopadhyay, D. Donadio, W. E. Pickett, B. R. Ortiz, E. S. Toberer, S. M. Kauzlarich, High seebeck coefficient and unusually low thermal conductivity near ambient temperatures in layered compound $Yb_{2-x}Eu_xCdSb_2$, *Chemistry of Materials*, 2018, **30**, 484-493, doi: 10.1021/acs.chemmater.7b04517.

[10] J. Sun, D. J. Singh, Thermoelectric properties of AMg2X2, AZn2Sb2(a = Ca, Sr, Ba; X = Sb, Bi), and Ba2ZnX2(X = Sb, Bi) Zintl compounds, *Journal of Materials Chemistry A*, 2017, **5**, 8499-8509, doi: 10.1039/c6ta11234j.

[11] Z. Zhang, X. Wang, Y. Liu, C. Chen, H. Yao, L. Yin, X. Li, S. Li, F. Zhang, F. Bai, J. Sui, B. Yu, F. Cao, X. Liu, J. Mao, G. Xie, Q. Zhang, Balancing the anionic framework polarity for enhanced thermoelectric performance in $YbMg_2Sb2$ Zintl compounds, *Journal of Materiomics*, 2019, **5**, 583-589, doi: 10.1016/j.jmat.2019.08.002.

[12] Z. Zada, A. Laref, G. Murtaza, A. Zeb, A. Yar, First-principles calculations of electronic and magnetic properties of XMn_2Y_2 (X = Ca, Sr; Y = Sb, Bi) compounds, *International Journal of Modern Physics B*, 2019, **33**, 1950199, doi: 10.1142/s0217979219501996.

[13] X. Zhang, B. Zhang, K. L. Peng, X. C. Shen, G. T. Wu, Y. C. Yan, S. J. Luo, X. Lu, G. Y. Wang, H. S. Gu, X. Y. Zhou, Spontaneously promoted carrier mobility and strengthened phonon scattering in p-type YbZn2Sb2 via a nanocompositing approach, *Nano Energy*, 2018, **43**, 159-167, doi: 10.1016/j.nanoen.2017.11.019.

[14] A. Bhardwaj, A. Rajput, A. K. Shukla, J. J. Pulikkotil, A. K. Srivastava, A. Dhar, G. Gupta, S. Auluck, D. K. Misra, R. C. Budhani, Mg_3Sb2-based Zintl compound: a non-toxic, inexpensive and abundant thermoelectric material for power generation, *RSC Advances*, 2013, **3**, 8504, doi: 10.1039/c3ra40457a.

[15] J. Shuai, H. Geng, Y. Lan, Z. Zhu, C. Wang, Z. Liu, J. Bao, C.-W. Chu, J. Sui, Z. Ren, Higher thermoelectric performance of Zintl phases $(Eu_{0.5}Yb_{0.5})_{1-x}Ca_xMg_2Bi_2$ by band engineering and strain fluctuation, *Proceedings of the National Academy of Sciences of the United States of America*, 2016, **113**, E4125-4132, doi: 10.1073/pnas.1608794113.

[16] A. A. Khan, A. H. Reshak, Z. Zada, M. Saqib, Z. Abbas, M. Ismail, S. Zada, G. Murtaza, S. Ali, A. Laref, Thermoelectric, structural, electronic, magnetic, and thermodynamic properties of $CaZn_2Ge2$ compound, *The European Physical Journal Plus*, 2022, **137**, 351, doi: 10.1140/epjp/s13360-022-02577-y.

[17] S. Zheng, J. Li, J. Zhang, K. Jiang, X. Liu, C. Chang, X. Wang, Effect of Si addition on the electrochemical corrosion and passivation behavior of Fe-Cr-Mo-C-B-Ni-P metallic glasses, *Journal of Non-Crystalline Solids*, 2018, **493**, 33-40, doi: 10.1016/j.jnoncrysol.2018.04.036.

[18] I. Qayyum, F. Ur Rehman, M. Zahra, K. Batool, W. Shoukat, S. Arshad, S. Anwar, A. Raza, Z. Zada, Progressive innovations in advanced functional materials for emerging bio-electronics, drugs sensing and healthcare, *Journal of Drug and Alcohol Research*, 2023, **12**, 5, doi: 10.4303/JDAR/236244.

[19] S. Shakeel, P. Song, H. A. Alsalmah, G. Murtaza, T. Huang, Investigation of pressure-dependent electronic and optical properties of double perovskites Cs_2AgXY6 (X = Bi, In; Y = Cl, Br), *Journal of Inorganic and Organometallic Polymers and Materials*, 2024, **34**, 1040-1054, doi: 10.1007/s10904-023-02888-2.

[20] Z. Zada, H. Ullah, R. Zada, S. Zada, A. Laref, S. Azam, A. A. Khan, M. Irfan, Structure stability, half metallic

© Engineered Science Publisher LLC 2024

ferromagnetism, magneto-electronic and thermoelectric properties of new zintl XCr_2Bi2 (X=Ca, Sr) compounds for spintronic and renewable energy applications, *Physica B: Condensed Matter*, 2021, **607**, 412866, doi: 10.1016/j.physb.2021.412866.
[21] R. Bauernschmitt, R. Ahlrichs, Stability analysis for solutions of the closed shell Kohn–Sham equation, *The Journal of Chemical Physics*, 1996, **104**, 9047-9052, doi: 10.1063/1.471637.
[22] S. Park, S. Woo, E. J. Mele, H. Min, Semiclassical Boltzmann transport theory for multi-Weyl semimetals, *Physical Review B*, 2017, **95**, 161113, doi: 10.1103/physrevb.95.161113.
[23] A. F. May, M. A. McGuire, D. J. Singh, R. Custelcean, G. E. Jellison, Jr., Structure and properties of single crystalline $CaMg_2Bi2$, $EuMg_2Bi_2$, and $YbMg_2Bi_2$, *Inorganic Chemistry*, 2011, **50**, 11127-11133, doi: 10.1021/ic2016808.
[24] V. Lucarini, K. E. Peiponen, J. J. Saarinen, E. M. Vartiainen, Kramers-Kronig relations in optical materials research, Springer Science & Business Media, 2005, 110.
[25] G. Murtaza, I. Ahmad, B. Amin, A. Afaq, M. Maqbool, J. Maqssod, I. Khan, M. Zahid, Investigation of structural and optoelectronic properties of $BaThO_3$, *Optical Materials*, 2011, **33**, 553-557, doi: 10.1016/j.optmat.2010.10.052.
[26] G. Murtaza, I. Ahmad, B. Amin, A. Afaq, F. Ghafoor, A. Benamrani, Linear and nonlinear optical response of $Mg_xZn_{1-x}O$: a density functional study, *Physica B: Condensed Matter*, 2011, **406**, 2632-2636, doi: 10.1016/j.physb.2011.04.004.
[27] Y. Zhang, Y. He, H. Wang, L. Sun, Y. Su, Ultra-broadband mode size converter using on-chip metamaterial-based Luneburg lens, *ACS Photonics*, 2021, **8**, 202-208, doi: 10.1021/acsphotonics.0c01269.
[28] F. Yu, S. Yu, C. Li, Z. Li, F. Song, Z. Xu, Y. Zhu, C. Dai, X. Cao, Z. Zhang, Y. Liu, J. Qiu, Molecular engineering of biomimetic donor-acceptor conjugated microporous polymers with full-spectrum response and an unusual electronic shuttle for enhanced uranium(VI) photoreduction, *Chemical Engineering Journal*, 2023, **466**, 143285, doi: 10.1016/j.cej.2023.143285.
[29] A. Gani, O. Cheref, M. Ghezali, M. Rabah, A. H. Reshak, Y. Djaballah, H. Righi, D. Rached, A. Belasri, Mechanical stability and optoelectronic behavior of BeXP2 (X=Si and Ge) chalcopyrite, *Chinese Journal of Physics*, 2020, **64**, 174-182, doi: 10.1016/j.cjph.2020.01.007.
[30] L. Boumia, F. Dahmane, B. Doumi, D. P. Rai, S. A. Khandy, H. Khachai, H. Meradji, A. H. Reshak, R. Khenata, Structural, electronic and magnetic properties of new full Heusler alloys Rh_2CrZ (Z = Al, Ga, In): first-principles calculations, *Chinese Journal of Physics*, 2019, **59**, 281-290, doi: 10.1016/j.cjph.2019.04.002.
[31] K. Bougherara, D. P. Rai, A. H. Reshak, First principles prediction of the elastic, electronic and optical properties of Sn3X4 (X = P, As, Sb, Bi) compounds: potential photovoltaic absorbers, *Chinese Journal of Physics*, 2019, **59**, 265-272, doi: 10.1016/j.cjph.2019.03.012.

Publisher's Note: Engineered Science Publisher remains neutral with regard to jurisdictional claims in published maps and institutional affiliations.

© Engineered Science Publisher LLC 2024